Elastic Fields of Quantum Dots in Multilayered Semiconductors: A Novel Green's Function Approach

B. Yang[1]
Structures Technology, Inc.,
543 Keisler Drive, Suite 204,
Cary, NC 27511
e-mail: boyang@boulder.nist.gov
Mem. ASME

E. Pan
Department of Civil Engineering,
University of Akron,
Akron, OH 44325
Mem. ASME

We present an efficient and accurate continuum-mechanics approach to predict the elastic fields in multilayered semiconductors due to buried quantum dots (QDs). Our approach is based on a novel Green's function solution in anisotropic and linearly elastic multilayers, derived within the framework of generalized Stroh formalism and Fourier transforms, in conjunction with the Betti's reciprocal theorem. By using this approach, the induced elastic fields due to QDs with general misfit strains are expressed as a volume integral over the QDs domains. For QDs with uniform misfit strains, the volume integral involved is reduced to a surface integral over the QDs boundaries. Further, for QDs that can be modeled as point sources, the induced elastic fields are then derived as a sum of the point-force Green's functions. In the last case, the solution of the QD-induced elastic field is analytical, involving no numerical integration, except for the evaluation of the Green's functions. As numerical examples, we have studied a multilayered semiconductor system of QDs made of alternating GaAs-spacer and InAs-wetting layers on a GaAs substrate, plus a freshly deposited InAs-wetting layer on the top. The effects of vertical and horizontal arrays of QDs and of thickness of the top wetting layer on the QD-induced elastic fields are examined and some new features are observed that may be of interest to the designers of semiconductor QD superlattices. [DOI: 10.1115/1.1544540]

1 Introduction

Owing to their great advantages over those processed by lithography and etching, self-assembled quantum semiconductor heterostructures have attracted tremendous attention in recent years. The processing of the heterostructures is based on the spontaneous growth of small islands from a wetting layer due to its mismatch strain to the substrate, i.e., a Stranski-Krastanow growth mechanism. The islands include quasi-zero-dimensional dots (or quantum dots (QDs)) and quasi-one-dimensional wires, on the scale of 1–100 nanometers. Experimental studies have shown that such QD nanostructures possess certain special electronic and optical features, rendering fascinating and novel devices, such as the low-threshold laser, resonant tunneling device, and huge-capacity memory media, possible, [1,2]. These features are in part related to the strain fields induced by the QDs and thus it is important to understand the latter before the design of devices, [1–3]. In their device applications, it is often desirable to fabricate the QDs in successive stacks with both vertical and lateral orderings, [4–8]. The final product is then a multilayered structure with buried arrays of QDs and with each layer being anisotropic. Therefore, an efficient and accurate numerical tool for predicting the mechanical fields, based on the theory of generally anisotropic elasticity for layered media, would be much appreciated.

To quantitatively explain and numerically model the QD nanostructures, various numerical methods have been proposed, including the continuum finite element (FE) and finite difference (FD) methods, [9–14], and the discrete atomic-level simulations, [15–17]. However, the domain-based FE and FD methods and the atomic models are computationally expensive, making them difficult to perform parametric studies in order to interpret the experimental phenomena or to reach an economic design strategy. This difficulty is manifested especially in the case of multilayered heterostructures. Recently, various analytical and semi-analytical methods, in particular, those related to the Green's function solutions, have been proposed and applied to the QD modeling, [18,19]. Because of their robust features in terms of accuracy and efficiency, these analytical methods, particularly the Green's function method, have been found to be very useful in the study of QD structures, [18–24]. For QDs in a three-dimensional isotropic infinite space, Pearson and Faux [23] derived the exact-closed-form solution for the QD-induced strain when the QDs are in the form of pyramids. When the infinite domain is anisotropic, Faux and Pearson [19] and Andreev et al. [22] derived the induced strain using, respectively, the Fourier transform method and the series expansion method. More recently, Pan and Yang [24] examined the elastic field due to a buried QD in an anisotropic half-space substrate using the point-force Green's function, which is derived within the framework of generalized Stroh formalism and Fourier transforms, in conjunction with the Betti's reciprocal theorem. Their result has shown clearly the effects of material anisotropy and free surface on the elastic fields.

In this paper, we propose a novel Green's function approach for the elastic analyses of buried QDs in multilayered semiconductors, advanced from the authors' previous works, [24,25]. The QDs and surrounding matrix are assumed to have the same material property, within the classical inclusion approach of eigenstrain, [26]. In this approach, the elastic fields induced by QDs with general misfit strains (i.e., eigenstrains) are expressed as a volume integral over the QDs domains. For QDs with a uniform misfit strain, the volume integral can be reduced to a surface integral over the QDs boundaries. Further, for QDs that can be modeled as point sources, the induced elastic fields can then be derived as a sum of the point-force Green's functions. In the last case, the QD solution is analytical, except for the numerical evaluation of the point-force Green's functions. The proposed approach then is applied to examine a multilayered system of QDs with alternating GaAs-spacer and InAs-wetting layers on a GaAs sub-

[1]To whom correspondence should be addressed. Present address: Materials Reliability Division, National Institute of Standards and Technology, Boulder, CO 80305.

Contributed by the Applied Mechanics Division of THE AMERICAN SOCIETY OF MECHANICAL ENGINEERS for publication in the ASME JOURNAL OF APPLIED MECHANICS. Manuscript received by the Applied Mechanics Division, Dec. 16, 2001; final revision, June 8, 2002. Associate Editor: H. Gao. Discussion on the paper should be addressed to the Editor, Prof. Robert M. McMeeking, Chair, Department of Mechanics and Environmental Engineering, University of California–Santa Barbara, Santa Barbara, CA 93106-5070, and will be accepted until four months after final publication in the paper itself in the ASME JOURNAL OF APPLIED MECHANICS.

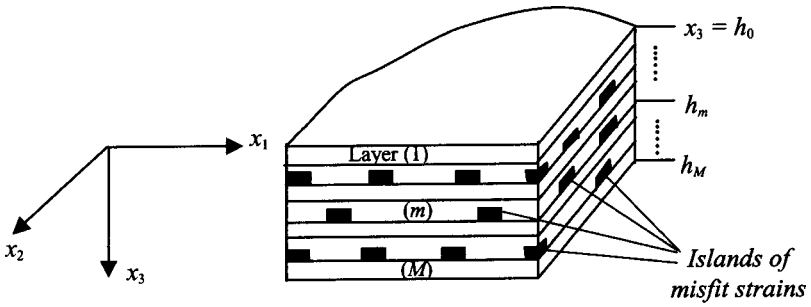

Fig. 1 A multilayered heterostructure with embedded islands of misfit strains

strate, plus a ''freshly'' deposited wetting layer on the top. The theory is described in Section 2. The numerical results are presented and discussed in Section 3. Conclusions are drawn in Section 4.

2 Theory

2.1 Integral Equation Formulation of Quantum Dots. Inclusion problem of misfit strains, [26], in a heterogeneous, anisotropic, linearly elastic matrix can be described in terms of an integral-equation formulation with the integral kernel being the point-force Green's function in the same media. This integral-equation formulation is a consequence of the Betti's reciprocal theorem. Let us assume that there are two states associated with the matrix domain D: one for the misfit-strain problem due to a given misfit strain $\varepsilon^0_{ij}(\mathbf{x})$, and the other for the Green's function problem due to a point force at $\mathbf{y}$. In these two problems, the boundary conditions along ∂D (boundary of D) are identical. Applying the Betti's reciprocal theorem, we find that the displacement $u_p(\mathbf{y})$ due to the misfit strain $\varepsilon^0_{ij}(\mathbf{x})$ can be expressed in terms of the following integral-equation formulation, as, [26],

$$u_p(\mathbf{y}) = \int_D u^*_{pi}(\mathbf{x};\mathbf{y})[-C_{ijlm}(\mathbf{x})\varepsilon^0_{lm}(\mathbf{x})]_{,j} dV(\mathbf{x}), \tag{1}$$

where $u^*_{pi}(\mathbf{x};\mathbf{y})$ is the Green's ith displacement component at $\mathbf{x}$ due to a point force in the pth direction applied at $\mathbf{y}$, C_{ijlm} is the elastic stiffness, heterogeneous in general, and a repeated index implies the conventional summation over its range. Note that $_{,j}$ indicates the partial derivative with respect to field coordinate x_j while $_{,y_p}$ is used for the partial derivative with respect to source coordinate y_p. Making use of the Gauss theorem, Eq. (1) can be rewritten as

$$u_p(\mathbf{y}) = \int_D u^*_{pi,j}(\mathbf{x};\mathbf{y}) C_{ijlm}(\mathbf{x})\varepsilon^0_{lm}(\mathbf{x}) dV(\mathbf{x}) - \int_{\partial D} u^*_{pi}(\mathbf{x};\mathbf{y}) C_{ijlm}(\mathbf{x})\varepsilon^0_{lm}(\mathbf{x}) n_j(\mathbf{x}) d\Gamma(\mathbf{x}), \tag{2}$$

where n_j is the outward normal at a boundary point.

We now consider a special heterogeneous matrix structure and a special misfit strain distribution, as shown in Fig. 1. The special heterogeneous matrix structure consists of multiple planar layers of different media. They are homogeneous, anisotropic, and linearly elastic. The special misfit-strain field is nonzero only in a number of interior islands $\Omega^{(n)}(n=1,\ldots,N)$. To apply the above theory, we assume that the islands have the same elastic property as their surrounding layer media. This special system represents a multilayered semiconductor with coherently strained QDs, [1]. We remark that there should exist nonzero eigenstrain field in some of the layers (i.e., wetting layers from which the QDs grow), similar to that in the QDs. In this case, the elastic field to be derived under the above assumption of nonzero eigenstrain only in the QDs is in fact the part of a total field induced by the QDs. The total field can be obtained by applying the rule of superposition of the induced field to the homogeneous field that is caused by the nonzero matrix eigenstrain alone (i.e., in the absence of the QDs) under the same boundary and interfacial conditions. For the present multilayered structure, the homogeneous elastic field can be solved by applying the classical laminate theory, [27].

Under these assumptions, Eq. (2) can be simplified. First, by using the fact that the misfit strain along the domain boundary ∂D is zero, the term of boundary integral in Eq. (2) is eliminated, which yields

$$u_p(\mathbf{y}) = \int_D u^*_{pi,j}(\mathbf{x};\mathbf{y}) C_{ijlm}(\mathbf{x})\varepsilon^0_{lm}(\mathbf{x}) dV(\mathbf{x}). \tag{3}$$

Then, reducing the integral domain from D to $\Omega^{(n)}(n=1,\ldots,N)$, Eq. (3) is rewritten as

$$u_p(\mathbf{y}) = \sum_{n=1}^{N} \int_{\Omega^{(n)}} u^*_{pi,j}(\mathbf{x};\mathbf{y}) C_{ijlm}(\mathbf{x})\varepsilon^0_{lm}(\mathbf{x}) dV(\mathbf{x}). \tag{4}$$

Further, the domain integrals in Eq. (4) can be reduced to the surface of $\Omega^{(n)}$ for those QDs in which the misfit strain distribution is uniform. Assuming that all of the islands have a uniform misfit strain field, we arrive at

$$u_p(\mathbf{y}) = \sum_{n=1}^{N} C^{(n)}_{ijlm}\varepsilon^{0(n)}_{lm} \int_{\partial\Omega^{(n)}} u^*_{pi}(\mathbf{x};\mathbf{y}) n_j(\mathbf{x}) dS(\mathbf{x}), \tag{5}$$

where $C^{(n)}_{ijlm}$ and $\varepsilon^{0(n)}_{lm}$ are, respectively, the (uniform) elastic stiffness and misfit strain in the nth island. Note that a uniform distribution of misfit strain in a QD may occur when the QD and matrix (generally mismatched in thermal expansion coefficients) are subjected to a uniform temperature change and if their mismatch of elastic constants can be neglected.

In order to find the induced elastic strain field, the displacement in Eq. (5) is differentiated with respect to the observation point $\mathbf{y}$ (i.e., the source point where the point force is located in the corresponding Green's function problem), which yields

$$\varepsilon^*_{pq}(\mathbf{y}) = \sum_{n=1}^{N} \frac{1}{2} C^{(n)}_{ijlm}\varepsilon^{0(n)}_{lm} \int_{\partial\Omega^{(n)}} [u^*_{pi,y_q}(\mathbf{x};\mathbf{y}) + u^*_{qi,y_p}(\mathbf{x};\mathbf{y})] n_j(\mathbf{x}) dS(\mathbf{x}). \tag{6}$$

Subsequently, the stress field is obtained as

$$\sigma_{pq}(\mathbf{y}) = C_{pqst}(\mathbf{y})[\varepsilon_{st}(\mathbf{y}) - \varepsilon^0_{st}(\mathbf{y})]. \tag{7}$$

Note that $\varepsilon^0_{st}(\mathbf{y})$ in Eq. (7) is nonzero only if $\mathbf{y}$ is within a QD.

Finally, the above expressions can be further reduced if the observation point $\mathbf{y}$ is remote to some or all of the QDs compared to their individual sizes. These remote QDs can be modeled as

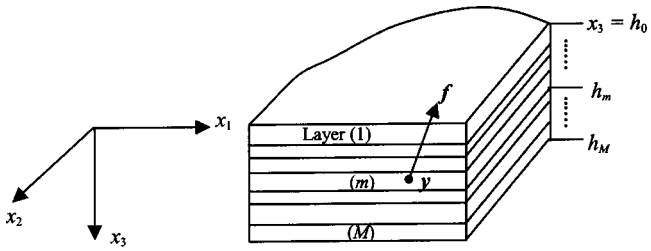

Fig. 2 Point-force Green's function problem of a multilayered heterostructure (Fig. 1)

point sources of misfit strain. Without the loss of generality, assuming the remoteness of **y** to all QDs, the misfit strain field is then expressed as

$$\varepsilon^0_{lm}(\mathbf{x}) = \sum_{n=1}^{N} \varepsilon^{0(n)}_{lm} V^{(n)} \delta(\mathbf{x} - \mathbf{x}^{(n)}), \tag{8}$$

where $V^{(n)}$ and $\mathbf{x}^{(n)}$ are, respectively, the volume and location of the nth QD, and $\delta(\mathbf{x})$ is the Dirac delta function. By substituting Eq. (8) in Eq. (3), the induced displacement and strain at **y** due to the point sources of misfit strain are analytically found to be

$$u_p(\mathbf{y}) = \sum_{n=1}^{N} u^*_{pi,j}(\mathbf{x}^{(n)};\mathbf{y}) C^{(n)}_{ijlm} \varepsilon^{0(n)}_{lm} V^{(n)}$$

$$= \sum_{n=1}^{N} \sigma^*_{plm}(\mathbf{x}^{(n)};\mathbf{y}) \varepsilon^{0(n)}_{lm} V^{(n)}, \tag{9}$$

$$\varepsilon_{pq}(\mathbf{y}) = \sum_{n=1}^{N} \frac{1}{2} [\sigma^*_{plm,y_q}(\mathbf{x}^{(n)};\mathbf{y}) + \sigma^*_{qlm,y_p}(\mathbf{x}^{(n)};\mathbf{y})] \varepsilon^{0(n)}_{lm} V^{(n)}. \tag{10}$$

In the derivation of the right-hand side of Eq. (9), the Hooke's law, $\sigma_{lm} = C_{ijlm} u_{i,j}$, was effected. It is observed in Eq. (9) that the displacement field in the pth direction at **y** due to point sources of misfit strain with components (lm) at $\mathbf{x}^{(n)}$ $(n = 1, \ldots, N)$ is equivalent to the stress field with components (lm) at $\mathbf{x}^{(n)}$ due to a point force in the pth direction at **y**, [28].

We remark that Eqs. (4), (5), and (9) (and their corresponding expressions for strain and stress) can be used whenever and wherever applicable to most efficiently compute the elastic fields due to a QD. The idea of applying the point-source approach to describe the elastic field remote to a QD, the inclusion approach to describe the field in an intermediate distance to a QD, and the imhomogeneity approach to describe the field close to or inside a QD, has been elaborated recently by Romanov et al. [29]. The different approaches require different computational tools to efficiently and accurately solve the problem. The present work proposes to apply a special Green's function for anisotropic multilayers to solve the problem of QDs approached as inclusions. It enables a simulation of a relatively large system of QDs in multilayered semiconductors. This special Green's function is described next.

2.2 Green's Function for Anisotropic Multilayers. Three-dimensional point-force Green's function in anisotropic multilayers, as shown in Fig. 2, can be solved within the framework of generalized Stroh formalism and Fourier transforms, [25,30]. The elegancy of the formulation has been demonstrated by applying the derived Green's functions to the boundary element analyses of stress around a hole in a composite laminate, [31], and the corresponding delamination crack problem, [32]. In the following, we summarize the Green's functions for anisotropic elastostatic multilayers. For details of the theory, one may refer to the authors' previous work, [25], and articles cited therein.

The equilibrium of a multilayered system subjected to a point force requires that

$$C_{pjlm}(\mathbf{x}) u_{l,mj}(\mathbf{x}) = -f_p \delta(\mathbf{x} - \mathbf{y}), \tag{11}$$

where f_p is the pth component of a point force applied at **y**. To solve this problem, the following two-dimensional Fourier transform (k_1, k_2) is first applied to the in-plane variables (x_1, x_2) of $u_i(x_1, x_2, x_3)$,

$$\tilde{u}_i(k_1, k_2, x_3) = \int \int u_i(x_1, x_2, x_3) e^{i x_\alpha k_\alpha} dx_1 dx_2, \tag{12}$$

where e stands for the *exponential* function, and i in the exponent denotes the unit of imaginary number, $\sqrt{-1}$, and the Greek index takes a value in the range from 1 to 2. The integral limits are $(-\infty, \infty)$ along both the coordinates x_1 and x_2. Thus, in the Fourier transformed domain, the governing Eq. (11) becomes

$$C_{p3i3}\tilde{u}_{i,33} - i(C_{p\alpha i3} + C_{p3i\alpha}) k_\alpha \tilde{u}_{i,3} - C_{p\alpha i\beta} k_\alpha k_\beta \tilde{u}_i = -f_p e^{i y_\alpha k_\alpha} \delta(x_3 - y_3), \tag{13}$$

which is valid for each individual homogeneous layer in the system.

Solving this ordinary differential equation in terms of x_3 with **f** being a unit force in the pth direction yields the general expression for the transformed-domain Green's displacement in the ith direction, $\tilde{u}^*_{ip}$, as

$$\tilde{\mathbf{u}}^*_m(x_3) = e^{i k_\alpha y_\alpha} [\tilde{\mathbf{u}}^{*(s)}_m(x_3) + i\eta^{-1} (\overline{\mathbf{A}}_m \langle e^{-i\overline{\mathbf{p}}_m \eta (x_3 - h_{m-1})} \rangle \mathbf{V}_m + \mathbf{A}_m \langle e^{-i\mathbf{p}_m \eta (x_3 - h_m)} \rangle \mathbf{W}_m)], \tag{14}$$

where the subscript m indicates the association of a quantity to the mth layer where the field point **x** resides; $\tilde{\mathbf{u}}^*_m$ is a function of k_1, k_2 and **y** as well as x_3; $\tilde{\mathbf{u}}^{*(s)}_m$, a special solution, is a given function of k_1, k_2 and **y** as well as x_3; and $\mathbf{V}_m$ and $\mathbf{W}_m$ are a pair of unknown tensors, being functions of k_1, k_2 and y_3, to be determined by imposing boundary and interfacial conditions. The dummy arguments in these functions, which are not relevant directly to the enforcement of boundary and interfacial conditions, are omitted for simplicity. In addition, the overbar denotes the complex conjugate, (η, θ) are the polar coordinates related to (k_1, k_2) by $k_1 = \eta \cos\theta$ and $k_2 = \eta \sin\theta$, and

$$\langle e^{-i\mathbf{p}\eta x_3} \rangle \equiv \mathrm{diag}[e^{-ip_1 \eta x_3}, e^{-ip_2 \eta x_3}, e^{-ip_3 \eta x_3}]. \tag{15}$$

In addition, **p** and $\mathbf{A} = (\mathbf{a}_1, \mathbf{a}_2, \mathbf{a}_3)$ are, respectively, the eigenvalues and eigenmatrix, related to each other by the following characteristic eigenrelation, [33–35], in an oblique plane spanned by $(n_1 = \cos\theta, n_2 = \sin\theta, 0)^T$ and $(0,0,1)^T$, as

$$[\mathbf{Q} + p_i(\mathbf{R} + \mathbf{R}^T) + p_i^2 \mathbf{T}] \mathbf{a}_i = 0, \tag{16}$$

with $Q_{ij} \equiv C_{i\alpha j\beta} n_\alpha n_\beta$, $R_{ij} \equiv C_{i\alpha j3} n_\alpha$, and $T_{ij} \equiv C_{i3j3}$.

Let us define **s** as a vector consisting of the in-plane stress components in the horizontal plane, and **t** as a vector consisting of the corresponding out-of-plane stress components. The combination of these two vectors represents the full stress tensor because of its symmetry. The corresponding Green's functions are given by $\mathbf{s}^* \equiv (\sigma^*_{11p}, \sigma^*_{12p}, \sigma^*_{22p})$ and $\mathbf{t}^* \equiv (\sigma^*_{13p}, \sigma^*_{23p}, \sigma^*_{33p})$, with subscript p indicating the unit point-force direction. By applying the Hooke's law, $\mathbf{t}^*$ and $\mathbf{s}^*$ can be derived from Eq. (14), in the transformed domain, as

$$\tilde{\mathbf{t}}^*_m(x_3) = e^{i k_\alpha y_\alpha} [\tilde{\mathbf{t}}^{*(s)}_m(x_3) + (\overline{\mathbf{B}}_m \langle e^{-i\overline{\mathbf{p}}_m \eta (x_3 - h_{m-1})} \rangle \mathbf{V}_m + \mathbf{B}_m \langle e^{-i\mathbf{p}_m \eta (x_3 - h_m)} \rangle \mathbf{W}_m)], \tag{17}$$

$$\tilde{\mathbf{s}}^*_m(x_3) = e^{i k_\alpha y_\alpha} [\tilde{\mathbf{s}}^{*(s)}_m(x_3) + (\overline{\mathbf{C}}_m \langle e^{-i\overline{\mathbf{p}}_m \eta (x_3 - h_{m-1})} \rangle \mathbf{V}_m + \mathbf{C}_m \langle e^{-i\mathbf{p}_m \eta (x_3 - h_m)} \rangle \mathbf{W}_m)], \tag{18}$$

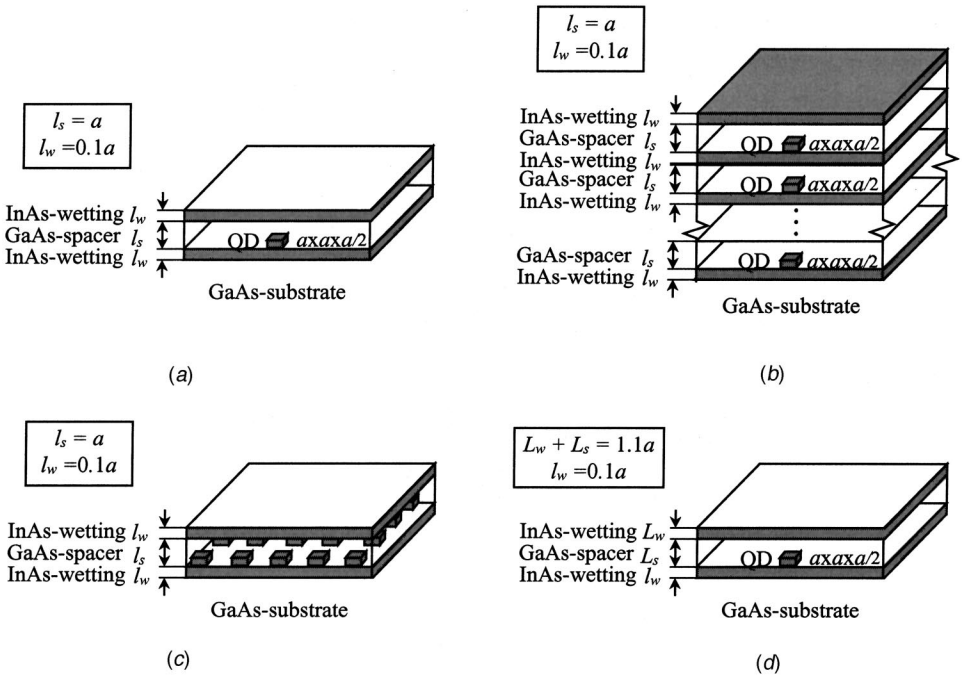

Fig. 3 Four examples of a heterostructure with alternating layers of GaAs-spacer and InAs-wetting on a GaAs substrate, plus a fresh wetting layer on the top: (*a*) a single QD; (*b*) a vertical array of QDs; (*c*) a horizontal rectangular array of QDs; (*d*) a single QD with varying ratio of thickness between top wetting and spacer layers

where $\tilde{\mathbf{t}}_m^{*(s)}$ and $\tilde{\mathbf{s}}_m^{*(s)}$ are derived from $\tilde{\mathbf{u}}_m^{*(s)}$ and matrix $\mathbf{B}$ and $\mathbf{C}$ are related to $\mathbf{A}$ and $\mathbf{p}$, [35]. The matrix $\mathbf{C}$ here is different from the fourth-rank tensor of elastic stiffness C_{ijkl}.

The derivatives of $\tilde{\mathbf{u}}^*$, $\tilde{\mathbf{t}}^*$, and $\tilde{\mathbf{s}}^*$ with respect to source coordinates $\mathbf{y}$ can be obtained from the above expressions, as

$$\tilde{\mathbf{u}}^*_{m,y_\alpha}(x_3) = ik_\alpha \tilde{\mathbf{u}}^*_m(x_3), \quad \tilde{\mathbf{t}}^*_{m,y_\alpha}(x_3) = ik_\alpha \tilde{\mathbf{t}}^*_m(x_3),$$
$$\tilde{\mathbf{s}}^*_{m,y_\alpha}(x_3) = ik_\alpha \tilde{\mathbf{s}}^*_m(x_3), \tag{19}$$

$$\tilde{\mathbf{u}}^*_{m,y_3}(x_3) = e^{ik_\alpha y_\alpha}[\tilde{\mathbf{u}}^{*(s)}_{m,y_3}(x_3) + i\eta^{-1}(\overline{\mathbf{A}}_m\langle e^{-i\overline{\mathbf{p}}_m\eta(x_3-h_{m-1})}\rangle \mathbf{V}'_m + \mathbf{A}_m\langle e^{-i\mathbf{p}_m\eta(x_3-h_m)}\rangle \mathbf{W}'_m)], \tag{20}$$

$$\tilde{\mathbf{t}}^*_{m,y_3}(x_3) = e^{ik_\alpha y_\alpha}[\tilde{\mathbf{t}}^{*(s)}_{m,y_3}(x_3) + (\overline{\mathbf{B}}_m\langle e^{-i\overline{\mathbf{p}}_m\eta(x_3-h_{m-1})}\rangle \mathbf{V}'_m + \mathbf{B}_m\langle e^{-i\mathbf{p}_m\eta(x_3-h_m)}\rangle \mathbf{W}'_m)], \tag{21}$$

$$\tilde{\mathbf{s}}^*_{m,y_3}(x_3) = e^{ik_\alpha y_\alpha}[\tilde{\mathbf{s}}^{*(s)}_{m,y_3}(x_3) + (\overline{\mathbf{C}}_m\langle e^{-i\overline{\mathbf{p}}_m\eta(x_3-h_{m-1})}\rangle \mathbf{V}'_m + \mathbf{C}_m\langle e^{-i\mathbf{p}_m\eta(x_3-h_m)}\rangle \mathbf{W}'_m)], \tag{22}$$

where $\mathbf{V}'_m$ and $\mathbf{W}'_m$ are a new pair of unknown tensors, as a function of k_1, k_2 and y_3.

The above unknown tensors $\mathbf{V}_m$, $\mathbf{W}_m$, $\mathbf{V}'_m$, and $\mathbf{W}'_m$ can be solved by imposing appropriate boundary and interfacial conditions provided that the special solutions are given. Yang and Pan [25] took the first few terms of the expansion solution of trimaterials, [36], to be the special solutions and solved the problem with traction-free top-boundary and symmetric bottom-boundary conditions and with the perfectly bonded interfacial conditions. The special solutions may also be taken as the infinite-space Green's function, [37], or the bimaterials solution, [30]. The difference would be in the resulting efficiency in evaluating the physical-domain Green's functions, [25]. By applying the boundary and interfacial conditions to the multilayers, a linear system of equations with the same number of unknowns can be formed and solved for each set of (k_1, k_2) in the transformed plane. Then, the physical-domain Green's functions are obtained by using the Fourier inverse transform, for example, the displacement field, as

$$u_i(x_1,x_2,x_3) = \frac{1}{(2\pi)^2}\int\int \tilde{u}_i(k_1,k_2,x_3)e^{-ix_\alpha k_\alpha}dk_1dk_2, \tag{23}$$

where the integral limits in both k_1 and k_2 are $(-\infty,\infty)$.

Above, we have only described the key steps in the derivation of the three-dimensional Green's functions for anisotropic elastostatic multilayers within the framework of generalized Stroh formalism and Fourier transforms. For details of the theory and relevant computational issues, one may refer to [25,30,35,36], and articles cited therein.

3 Results and Discussions

In this section, we apply the integral-equation formulation, described in the previous section, to investigate the elastic fields due to embedded QDs in a multilayered semiconductor system. Effects of vertical and lateral orderings of QDs and of thickness of wetting layer on the elastic fields will be addressed. The multilayered semiconductor consists of up to four sets of alternating GaAs-spacer and InAs-wetting layers on a GaAs substrate, plus a ''freshly'' deposited InAs-wetting layer on the top. Four different examples as shown in Figs. 3(*a–d*) are studied. The top surface is assumed to be traction-free while the interfaces are in the perfect-bonding condition. The far-field stress and displacement are zero. The thickness of the wetting and spacer layers is denoted by l_w and l_s, respectively. It is taken that $l_w = 0.1a$ and $l_s = a$ with the exception in the last example (Fig. 3(*d*)). The QDs are assumed to be cuboidal with dimensions $a \times a \times a/2$. They are seated on the top of a wetting layer and embedded in the above adjacent GaAs-spacer, as shown in Fig. 3(*a–d*). It is mentioned that the sides of the QDs are taken to be along the global coordinates (x_1, x_2, x_3). For simplicity, we also assume that the QDs have the same elastic property as its surrounding GaAs-spacer, and the misfit strain in the QDs is hydrostatic, i.e., $\varepsilon^0_{ij} = \varepsilon^0 \delta_{ij}$. The elastic constants for

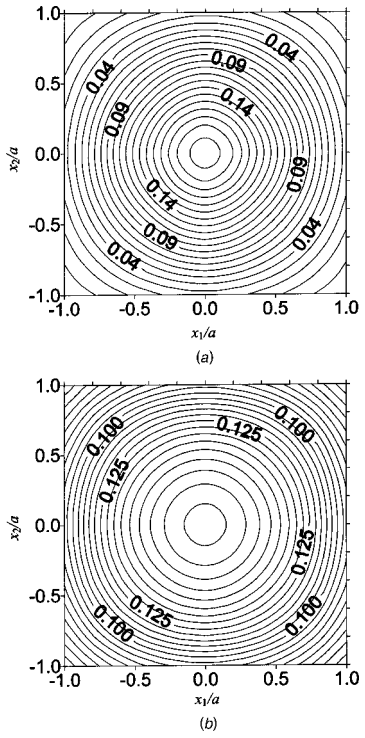

Fig. 4 Elastic fields on top surface induced by a single QD (Fig. 3*a*): (*a*) normalized hydrostatic strain $\varepsilon_{kk}/\varepsilon^0$; (*b*) normalized vertical displacement component $-u_3/(\varepsilon^0 a)$

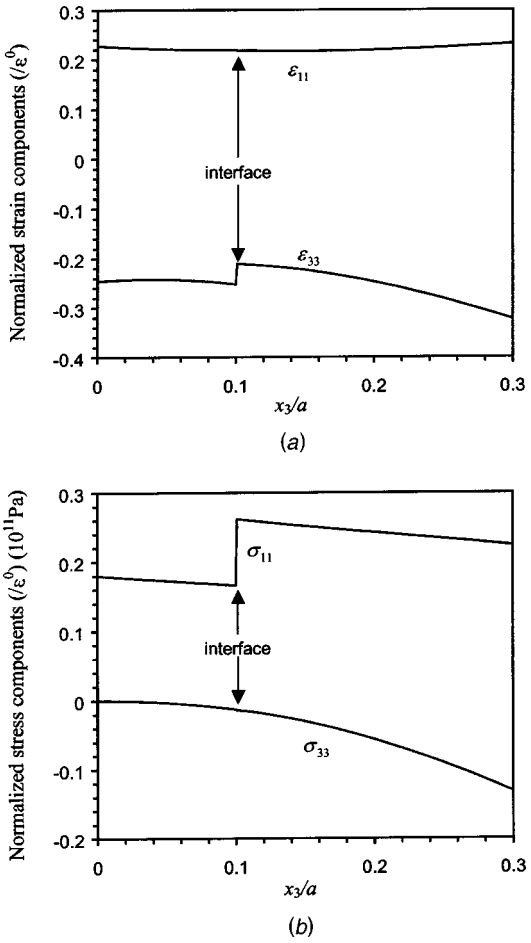

Fig. 5 Vertical variation of normalized nonzero strain and stress components over a single QD (Fig. 3*a*): (*a*) $\varepsilon_{11}(\varepsilon_{22}=\varepsilon_{11})$ and $\varepsilon_{33}/\varepsilon^0$; (*b*) $\sigma_{11}(\sigma_{22}=\sigma_{11})$ and $\sigma_{33}/\varepsilon^0$ in 10^{11} Pa

GaAs are $C_{11}=118$, $C_{12}=54$, $C_{44}=59$ and for InAs $C_{11}=83$, $C_{12}=45$, $C_{44}=40$ (GPa), with their crystallographic directions [100], [010], and [001] coinciding with the global coordinates x_1, x_2, and x_3, respectively. We remark that there should exist nonzero eigenstrain in the wetting layers, similar to that in the QDs. Because of the linearity of the problem, the QD-induced elastic field discussed below and the homogenous field due to the nonzero eigenstrain in the wetting layers can be superposed. In the present multilayer structure, the homogenous field can be obtained by applying the classical laminate theory, [27].

3.1 Example 1: A Single Quantum Dot. A buried single QD in the layered semiconductor system of top-InAs-wetting/GaAs-spacer/InAs-wetting/GaAs-substrate, as shown in Fig. 3(*a*), is first studied. The cuboidal QD is seated on the top of the internal wetting layer and embedded in the spacer, with its center located at $(0,0,0.85a)$. The top InAs layer represents a "freshly" deposited wetting layer where a next generation of QDs is expected to grow. Figures 4(*a*) and 4(*b*) show, respectively, the contour plots of the normalized hydrostatic strain $\varepsilon_{kk}/\varepsilon^0$ and normalized vertical displacement $-u_3/(\varepsilon^0 a)$ on the top surface (i.e., the free surface of the freshly deposited InAs-wetting layer) above the QD. Figure 5 shows the vertical variation of the normalized nonzero strain and stress components over the center of the QD. It is noted that, in this example, only the diagonal components, ε_{11}, $\varepsilon_{22}(=\varepsilon_{11})$, ε_{33}, σ_{11}, $\sigma_{22}(=\sigma_{11})$, and σ_{33}, are nonzero.

It is observed from Fig. 4 that due to the coincidence of the crystallographic orientations of the wetting and spacer crystals with the side orientations of the cuboidal QD, the normalized hydrostatic strain and vertical displacement are symmetric relative to the in-plane axes. They reach their maximum values at the origin, (0,0,0), right above the QD center on the free surface. We remark, however, that should the GaAs (111) be used in place of GaAs (001) for the spacer, the contour plots will be distorted with completely different features. The characteristics may be correlated to the electronic and optical behaviors of the semiconductor system, and to the growth direction and vertical correlation of new QDs, [38,39].

Due to the mismatch between the wetting and spacer layer crystals, the out-of-plane strain component, ε_{33}, and the in-plane stress components, σ_{11} and σ_{22}, are discontinuous across the interface, as shown in Fig. 5. However, the other in-plane strain and out-of-plane stress components, as well as all the displacement components, are continuous, as enforced in the Green's function solution, and in turn reflected in the inclusion solution of eigenstrains, [26]. It is also interesting to note from Fig. 5 that in the wetting layer, the magnitude of the in-plane strain and stress components increases when the observation point approaches the traction-free top surface, a phenomenon that may be explained by the free-surface bending effect.

3.2 Example 2: A Vertical Array of Quantum Dots. Effect of a vertical array of QDs on the elastic fields is examined in this example. Figure 3(*b*) schematically shows the geometry of the problem. Simulations were performed with repeated sets of alternating spacer and wetting layers with a QD embedded in each set. The variation of the normalized hydrostatic strain and vertical displacement along a line $(x_1,0,0)$ on the top surface is shown in Figs. 6(*a*) and 6(*b*). In these two figures, the results for *n* QD correspond to a semiconductor model made of *n* set of GaAs/InAs (plus a fresh InAs on the top and a GaAs substrate on the bottom). For instance, the results for one QD correspond to a semiconductor model with only one set of GaAs/InAs (plus a fresh InAs on the top and a GaAs substrate on the bottom, exactly the same as in

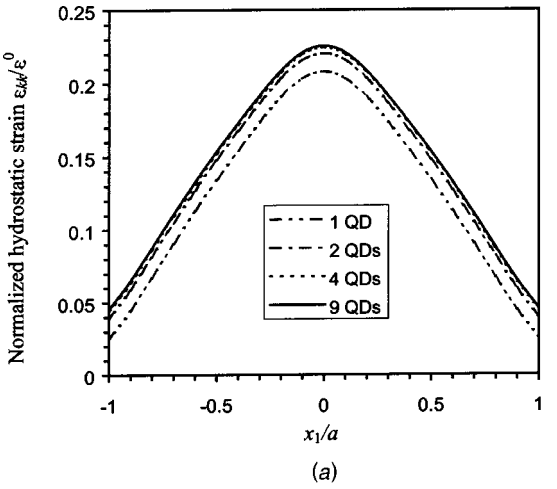

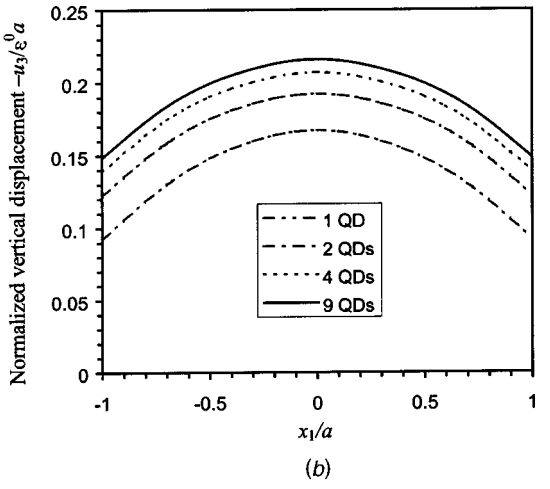

Fig. 6 Induced elastic fields along a line $(x_1,0,0)$ on top surface due to a vertical array of up to nine QDs (Fig. 3*b*): (*a*) normalized hydrostatic strain $\varepsilon_{kk}/\varepsilon^0$; (*b*) normalized vertical displacement component $-u_3/(\varepsilon^0 a)$

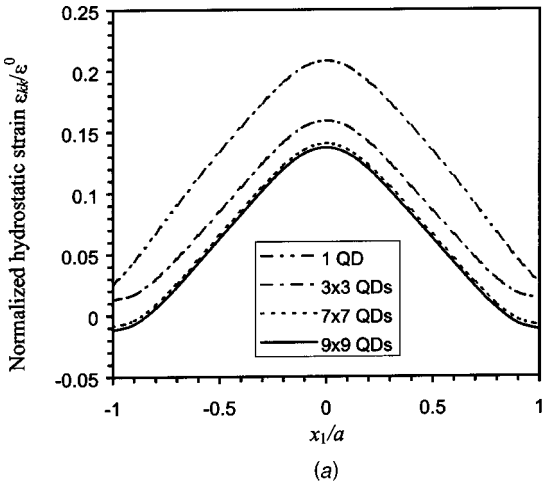

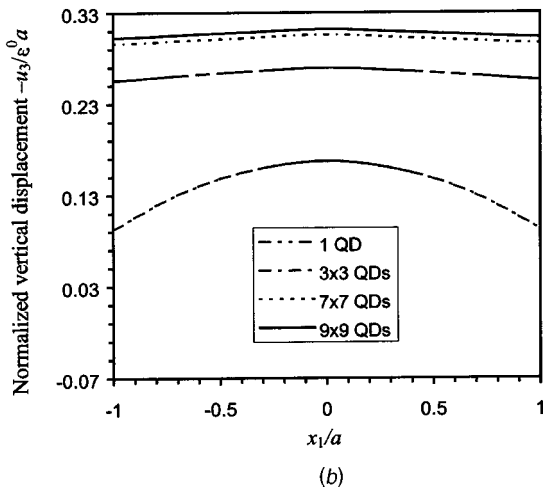

Fig. 7 Induced elastic fields along a line $(x_1,0,0)$ on top surface due to a horizontal rectangular array of up to 9×9 QDs (Fig. 3*c*): (*a*) normalized hydrostatic strain $\varepsilon_{kk}/\varepsilon^0$; (*b*) normalized vertical displacement component $-u_3/(\varepsilon^0 a)$

the previous case), and results for four QDs correspond to a semiconductor model consisting of four sets of GaAs/InAs, i.e., top-InAs/GaAs/InAs/GaAs/InAs/GaAs/InAs/GaAs-substrate, with a QD in each GaAs-spacer layer.

It can be observed from Fig. 6(*a*) that the magnitude of the hydrostatic strain on the surface increases with increasing number of QDs and converges quickly to the maximum values. This suggests that a vertical array of QDs should sum up their effects of elastic relaxation on the freshly deposited wetting layer (top wetting layer) where a new generation of QDs is expected to grow. The displacement field, on the contrary, has not shown its tendency of convergence with the number of QDs of the vertical array so far.

3.3 Example 3: A Horizontal Array of Quantum Dots. Now, effect of a horizontal array of QDs on the elastic fields is studied. Simulations were performed with a horizontal rectangular array of QDs located in the spacer. The semiconductor system consists of only one set of alternating spacer and wetting layers, as shown in Fig. 3(*c*). The spacing between the adjacent QDs (from center to center) in both in-plane directions is $2a$, with size of array varying from 3×3 to 9×9. Variations of the normalized hydrostatic strain and vertical displacement on the surface above the central QD are plotted in Fig. 7.

These results show that, with increasing number of QDs laterally around the central one, the magnitude of the surface elastic-strain field decreases and converges to its minimum value. Therefore, the surrounding QDs in the lateral directions play a role in relaxing the induced elastic field due to the central QD, an effect opposite to that of a vertical array of QDs as observed earlier. Consequently, the existence of laterally neighboring QDs would suppress the effect of the central QD on the growth of a new QD above it. The vertical displacement component converges with increasing number of QDs, again in contrast to that in the case of a vertical array of QDs.

3.4 Example 4: A Single QD With Varied Thickness of Top Wetting Layer. At last, effect of top wetting layer thickness on the QD-induced elastic field is studied. The geometry is similar to that studied in the first example (Fig. 3(*a*)), but with varied thickness of the top-wetting layer and spacer layer. The total thickness of these two layers is fixed at $1.1a$, as shown in Fig. 3(*d*). Similar to that in the first example, a single QD is located at the bottom of the spacer layer. To distinguish this example from the previous ones, the varied thicknesses of the top wetting and spacer layers are now indicated by L_w and L_s, respectively. On the top surface at three locations (0,0,0), $(0.5a,0,0)$, and $(a,0,0)$, the normalized hydrostatic strain, $\varepsilon_{kk}/\varepsilon^0$, and vertical displacement component, $-u_3/(\varepsilon^0 a)$, are evaluated with various combinations of thickness

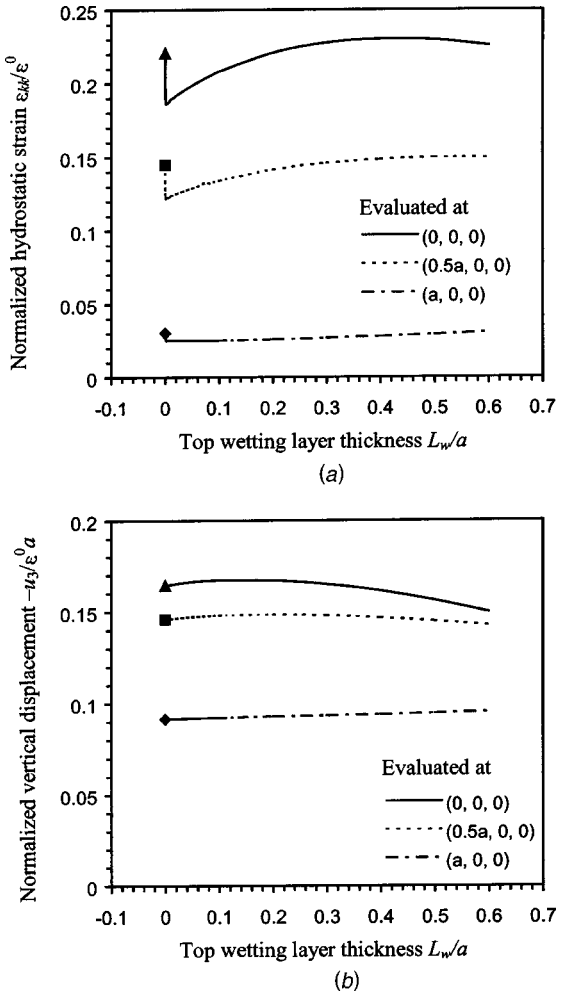

Fig. 8 Variation of elastic fields at three locations on top surface with top wetting layer thickness L_w (Fig. 3*d*): (*a*) normalized hydrostatic strain $\varepsilon_{kk}/\varepsilon^0$; (*b*) normalized vertical displacement component $-u_3/(\varepsilon^0 a)$. The results for the extreme case $L_w=0$ are indicated by symbols.

of these two layers. In addition, the extreme case without the top wetting layer (i.e., $L_w=0$) is solved. The results are shown in Fig. 8.

It can be seen that the variations of these quantities are continuous with thickness ratio between the top wetting and spacer layers. However, when $L_w=0$, the strain, as well as stress which is not shown, exhibits a jump. Meanwhile, the vertical displacement converges at $L_w=0$. The jumps in the strain and stress fields at $L_w=0$ are due to the material mismatch between the wetting and spacer layers. It is also observed that the variations of these QD-induced elastic fields may not be monotonic with the varying thickness ratio. This may be due not only to the materials mismatch between the wetting and spacer layers but also to the free-surface bending effect. Therefore, these elastic fields in the freshly deposited wetting layer cannot be modeled accurately by assigning identical elastic property to the wetting and spacer layers, no matter how thin the wetting layer is, in the multilayered semiconductor system of InAs and GaAs.

4 Conclusions

In this paper, we have proposed a novel Green's function approach to the elastic field in multilayered semiconductors with embedded coherently strained QDs. The problem of QDs with misfit strains is modeled as an anisotropic elastostatic inclusion problem of eigenstrains, [26]. The unique feature of the approach is that the point-force Green's function used for the multilayer system satisfies the boundary and interfacial-continuity conditions. By applying the Betti's reciprocal theorem, the elastic field induced by QDs with general misfit strains is expressed in terms of a domain integral with the point-force Green's function as integral kernel. The domain integral is reduced to a surface integral along the boundary of a QD that has a uniform misfit-strain distribution. Further, for QDs that can be modeled as point sources, the induced elastic field is then derived as a sum of the point-force Green's functions. These novel features make the present continuum-mechanics approach both accurate and efficient for carrying out a parametric study of QDs-induced elastic field in multilayered semiconductors.

By applying the Green's function approach, we have analyzed the elastic field due to embedded QDs in a system of alternating GaAs-spacer and InAs-wetting layers on a GaAs substrate, plus a freshly deposited InAs-wetting layer on the top. The QDs embedded in the spacer layers are assumed to have the same elastic constants as the spacer medium. The effects of vertical and horizontal arrays of QDs and of thickness of the top wetting layer on the elastic fields are examined and discussed in detail. The following features have been observed:

- First, the QD-induced out-of-plane strain and in-plane stress components exhibit discontinuities across the interface between the wetting and spacer layers due to the materials mismatch between these layers.
- Second, the magnitude of the induced in-plane strain and stress components increases when the observation point moves away from the QD source towards the top free surface. This may be explained by the free-surface bending effect.
- Third, a vertical array of QDs sums up their effects of elastic relaxation on the freshly deposited wetting layer, where a new generation of QDs is expected to grow. However, a horizontal array of QDs plays a role in deducting the elastic relaxation effect of the central QD on the top wetting layer, in contrast to that of a vertical array of QDs.
- Finally, when the thickness of the top wetting layer varies, the induced elastic field on the top surface changes continuously. However, when the top wetting layer totally disappears, some of the elastic strain and stress components exhibit a jump, due to the difference of elastic property between the wetting and spacer layers.

Acknowledgment

The authors would like to thank Dr. Vinod Tewary of the NIST at Boulder, Colorado for discussion and encouragement.

References

[1] Bimberg, D., Grundmann, M., and Ledentsov, N. N., 1998, *Quantum Dot Heterostructures*, John Wiley and Sons, New York.
[2] Brunner, K., 2002, "Si/Ge Nanostructures," Rep. Prog. Phys., **65**, pp. 27–72.
[3] Freund, L. B., and Johnson, H. T., 2001, "Influence of Strain on Functional Characteristics of Nanoelectronic Devices," J. Mech. Phys. Solids, **49**, pp. 1925–1935.
[4] Xie, Q., Madhukar, A., Chen, P., and Kobayashi, N. P., 1995, "Vertically Self-Organized InAs Quantum Box Islands on GaAs(100)," Phys. Rev. Lett., **75**, pp. 2542–2545.
[5] Tersoff, J., Teichert, C., and Lagally, M. G., 1996, "Self-Organization in Growth of Quantum Dot Supperlattices," Phys. Rev. Lett., **76**, pp. 1675–1678.
[6] Ishikawa, H., Shoji, H., Nakata, Y., Mukai, K., Sugawara, M., Egawa, M., Otsuka, N., Sujiyama, Y., Futatsugi, T., and Yokoyama, N., 1998, "Self-Organized Quantum Dots and Lasers," J. Vac. Sci. Technol. A, **16**, pp. 794–800.
[7] Springholz, G., Pinczolits, M., Holy, V., Zerlauth, S., Vavra, I., and Bauer, G., 2001, "Vertical and Lateral Ordering in Self-Organized Quantum Dot Supperlattices," Physica E (Amsterdam), **9**, pp. 149–163.
[8] Le Ru, E. C., Bennett, A. J., Roberts, C., and Murray, R., 2002, "Strain and Electronic Interactions in InAs/GaAs Quantum Dot Multilayers for 1300 nm Emission," J. Appl. Phys., **91**, pp. 1365–1370.
[9] Grundmann, M., Stier, O., and Bimberg, D., 1995, "InAs/GaAs Pyramidal

Quantum Dots: Strain Distribution, Optical Phonons, and Electronic Structure,'' Phys. Rev. B, **52**, pp. 11,969–11,981.
[10] Benabbas, T., Francois, P., Androussi, Y., and Lefebvre, A., 1996, ''Stress Relaxation in Highly Strained InAs/GaAs Structures as Studied by Finite Element Analysis and Transmission Electron Microscopy,'' J. Appl. Phys., **80**, pp. 2763–2767.
[11] Johnson, H. T., Freund, L. B., Akyuz, C. D., and Zaslavsky, A., 1998, ''Finite Element Analysis of Strain Effects on Electronic and Transport Properties in Quantum Dots and Wires,'' J. Appl. Phys., **84**, pp. 3714–3725.
[12] Kret, S., Benabbas, T., Delamarre, C., Androussi, Y., Dubon, A., Laval, J. Y., and Lefebvre, A., 1999, ''High Resolution Electron Microscope Analysis of Lattice Distortions and in Segregation in Highly Strained In0.35Ga0.65As Coherent Islands Grown on GaAs(001),'' J. Appl. Phys., **86**, pp. 1988–1993.
[13] Jogai, B., 2001, ''Three-Dimensional Strain Field Calculations in Multiple InN/AIN Wuutzite Quantum Dots,'' J. Appl. Phys., **90**, pp. 699–704.
[14] Johnson, H. T., and Freund, L. B., 2001, ''The Influence of Strain on Confined Electronic States in Semiconductor Quantum Structures,'' Int. J. Solids Struct., **38**, pp. 1045–1062.
[15] Daruka, I., Barabasi, A. L., Zhou, S. J., Germann, T. C., Lomdahl, P. S., and Bishop, A. R., 1999, ''Molecular-Dynamics Investigation of the Surface Stress Distribution in a Ge/Si Quantum Dot Superlattice,'' Phys. Rev. B, **60**, pp. R2150–R2153.
[16] Kikuchi, Y., Sugii, H., and Shintani, K., 2001, ''Strain Profiles in Pyramidal Quantum Dots by Means of Atomistic Simulation,'' J. Appl. Phys., **89**, pp. 1191–1196.
[17] Makeev, M. A., and Maduhukar, A., 2001, ''Simulations of Atomic Level Stresses in Systems of Buried Ge/Si Islands,'' Phys. Rev. Lett., **86**, pp. 5542–5545.
[18] Ru, C. Q., 1999, ''Analytic Solution for Eshelby's Problem of an Inclusion of Arbitrary Shape in a Plane or Half Plane,'' ASME J. Appl. Mech., **66**, pp. 315–322.
[19] Faux, D. A., and Pearson, G. S., 2000, ''Green's Tensors for Anisotropic Elasticity: Application to Quantum Dots,'' Phys. Rev. B, **62**, pp. R4798–R4801.
[20] Davies, J. H., 1998, ''Elastic and Piezoelcetric Fields around a Buried Quantum Dot: A Simple Picture,'' J. Appl. Phys., **84**, pp. 1358–1365.
[21] Davies, J. H., 1999, ''Quantum Dots Induced by Strain from Buried and Surface Stressors,'' Appl. Phys. Lett., **75**, pp. 4142–4144.
[22] Andreev, A. D., Downes, J. R., Faux, D. A., and O'Reilly, E. P., 1999, ''Strain Distributions in Quantum Dots of Arbitrary Shape,'' J. Appl. Phys., **86**, pp. 297–305.
[23] Pearson, G. S., and Faux, D. A., 2000, ''Analytical Solutions for Strain in Pyramidal Quantum Dots,'' J. Appl. Phys., **88**, pp. 730–736.
[24] Pan, E., and Yang, B., 2001, ''Elastostatic Fields in an Anisotropic Substrate due to a Buried Quantum Dot,'' J. Appl. Phys., **90**, pp. 6190–6196.
[25] Yang, B., and Pan, E., 2001, ''Efficient Evaluation of Three-Dimensional Green's Functions for Anisotropic Elastostatic Multilayered Composites,'' Eng. Anal. Boundary Elem., **26**, pp. 355–366.
[26] Mura, T., 1987, *Micromechanics of Defects in Solids*, Martinus Nijhoff, Boston.
[27] Tsai, S. W., and Hahn, H. T., 1980, *Introduction to Composite Materials*, Technomic Publishing, Westport, CT.
[28] Pan, E., 1991, ''Dislocation in an Infinite Poroelastic Medium,'' Acta Mech., **87**, pp. 105–115.
[29] Romanov, A. E., Beltz, G. E., Fischer, W. T., Petroff, P. M., and Speck, J. S., 2001, ''Elastic Fields of Quantum Dots in Subsurface Layers,'' J. Appl. Phys., **89**, pp. 4523–4531.
[30] Pan, E., and Yuan, F. G., 2000, ''Three-Dimensional Green's Functions in Anisotropic Bimaterials,'' Int. J. Solids Struct., **37**, pp. 5329–5351.
[31] Pan, E., Yang, B., Cai, X., and Yuan, F. G., 2001, ''Stress Analyses Around Holes in Composite Laminates Using Boundary Element Method,'' Eng. Anal. Boundary Elem., **25**, pp. 31–40.
[32] Yang, B., 2002, ''Examination of Free-Edge Crack Nucleation Around an Open Hole in Composite Laminates,'' Int. J. Fract., **115**, pp. 173–191.
[33] Stroh, A. N., 1958, ''Dislocations and Cracks in Anisotropic Elasticity,'' Philos. Mag., **3**, pp. 625–646.
[34] Stroh, A. N., 1962, ''Steady State Problems in Anisotropic Elasticity,'' J. Math. Phys., **41**, pp. 77–103.
[35] Ting, T. C. T., 1996, *Anisotropic Elasticity*, Oxford University Press, Oxford, UK.
[36] Yang, B., and Pan, E., 2001, ''Three-Dimensional Green's Functions in Anisotropic Trimaterials,'' Int. J. Solids Struct., **39**, pp. 2235–2255.
[37] Tonon, F., Pan, E., and Amadei, B., 2001, ''Green's Functions and Boundary Element Formulation for 3D Anisotropic Media,'' Comput. Struct., **79**, pp. 469–482.
[38] Holy, V., Springholz, G., Pinezolits, M., and Bauer, G., 1999, ''Strain Induced Vertical and Lateral Correlations in Quantum Dot Superlattices,'' Phys. Rev. Lett., **83**, pp. 356–359.
[39] Harrison, P., 2000, *Quantum Wells, Wires and Dots: Theoretical and Computational Physics*, John Wiley and Sons, New York.